A STUDY OF THE EFFECT OF MOBILITY RATIOS ON PATTERN DISPLACEMENT BEHAVIOR AND STREAMLINES TO INFER PERMEABILITY FIELDS PERMEABILITY MEDIA

SUPRI TR 115

By

Yuandong Wang

Anthony R. Kovscek

William E. Brigham

December 1998

Work Performed Under Contract No. DE-FG22-96BC14994

Prepared for
U.S. Department of Energy
Assistant Secretary for Fossil Energy

Thomas Reid, Project Manager
National Petroleum Technology Office
P.O. Box 3628

TABLE OF CONTENTS

LIST OF FIGURES

Chapter 1

Chapter 2

ACKNOWLEDGMENTS

This work was supported by the Assistant Secretary for Fossil Energy, Office of Oil, Gas, and Shale Technologies of the U.S. Department of Energy under contract No. DE-FG22-96BC14994 to Stanford University. Likewise, the support of the SUPRI-A Industrial Affiliates is gratefully acknowledged.

ABSTRACT

In my MS research program I worked on two research topics. I finished the first research topic and conducted some preliminary research on the second topic. The second topic is actually a first step toward my Ph.D. program. Below is a brief description of my work on the two topics.

1. A study of the effect of mobility ratios on pattern displacement behavior

It is well known, for unit mobility ratio, that the areal sweep efficiency of a staggered line drive pattern is always better than a five-spot pattern. However, this observation does not hold for very favorable mobility ratios.

I studied the effect of mobility ratios on pattern behavior by the means of simulation using a streamline simulator. In this report, I present simulation results and, with the help of streamline and saturation distributions, explain the differences between displacements with unit and favorable mobility ratios. Simulations compare well with experiments conducted elsewhere.

Accurate definition of breakthrough time is also discussed for multiphase, streamline, simulation results. The exact definition of breakthrough is difficult due to physical dispersion in experiments and numerical dispersion in simulations.

2. Streamline approach to the inverse problem of inferring permeability distribution

It is often useful to infer the permeability field of a porous medium, such as an oil reservoir or a ground water aquifer from a tracer breakthrough curve at the production well. There are many approaches to this inverse problem, such as simulated annealing, sensitivity studies either analytical or numerical, genetic algorithms, and geo-statistical approaches. Most of these approaches are very time consuming.

An efficient approach is desirable. Here I propose an alternative approach—an inverse streamline approach. I have conducted some preliminary work on this topic, to be described later, and obtained some satisfactory results. These results indicate that this project is robust and promising. However, there are simplifications in my current study, such as piston-like displacement, unit mobility ratio and incompressible flow. If these simplifications can be relaxed, then this can be a very efficient approach to the inverse problem with broader applications.

1. EFFECT OF MOBILITY RATIO ON PATTERN BEHAVIOR OF A HOMOGENEOUS POROUS MEDIUM

1.1 INTRODUCTION

Pattern geometry plays a major role in determining oil recovery during secondary and enhanced oil recovery operations. Although simulation is an important tool for design and evaluation, the first step often involves rough calculations based upon areal sweep efficiencies of displacements in homogeneous, two-dimensional, scaled, physical models (Dyes *et al*., 1954; Craig, 1971; Lake, 1989). These results are available as a function of the displacement pattern and the mobility ratio, M. The mobility ratio is simply the mobility of the displacing phase over that of the displaced, or resident, phase. Because it is possible to compute sweep efficiency analytically when the displacing and displaced phase have the same mobility (Morel-Seytoux, 1966), scaled physical model results have been verified for unit mobility ratios.

Convincing verification of the non-unit mobility ratio cases does not appear in the literature. Typical finite difference solutions of the reservoir flow equations suffer from numerical dispersion, the effects of which are hard to evaluate. Furthermore, the scaled physical model results at low mobility ratios ($M << 1$) are provocative. For instance, Fig. 1a shows that recovery from a five-spot pattern at breakthrough for 1/M greater than about 6 is virtually 100%, whereas recovery at breakthrough in Fig. 1b for a staggered-line-drive pattern at an 1/M of 6 is only about 88.5%. This contradicts the common notion that areal sweep efficiency from a staggered-line-drive pattern is always better than that from a five-spot pattern.

We use a 3D streamline simulator (Batycky, *et al*., 1996) to analyze displacements in five-spot and staggered-line-drive patterns for stable displacements, that is M less than 1. In the following sections, we present streamline distributions, saturation distributions, and fractional flow at the producer versus dimensionless time, t_D. The dimensionless time is the pore volumes of displacing fluid injected. With the streamline

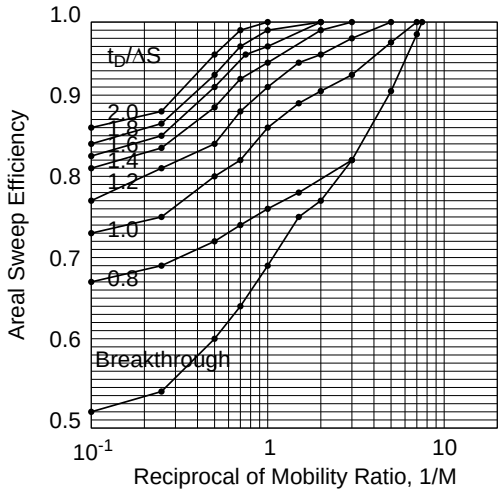

(a) Five Spot Pattern

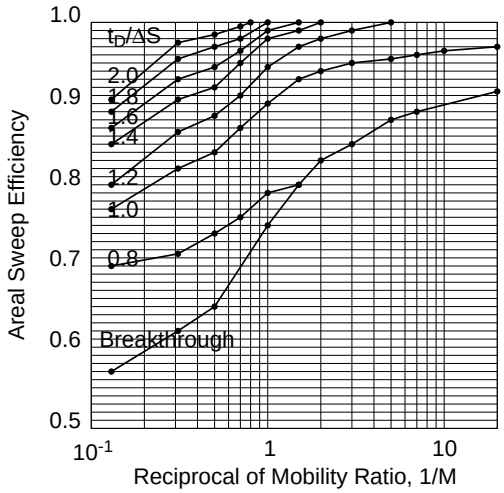

(b) Staggered Line Drive, d/a = 1

Fig 1 Dyes et al(1954) Experimental Results

and saturation distributions at different times, we explain why and at what mobility ratio the five spot pattern can recover more oil than a staggered line drive pattern.

The streamline calculation method is advantageous in that the results suffer from much less numerical dispersion than typical finite-difference approximations, but some dispersion in simulation results is evident. Therefore, we discuss how to treat the numerical dispersion to obtain accurate estimates of breakthrough times. We discuss the proper way to calculate fractional flow based on the flow rates at the producer. In comparing the simulation results with the experimental results of Dyes *et al.* (1954), physical dispersion in the experiments is found even though a piston-like displacement was assumed.

1.2 SWEEP EFFICIENCY

Before proceeding, it is useful to recall the representation of experimental data in Fig. 1 and the meaning of sweep efficiency. Dyes *et al*. (1954) used various oils as both the injected and displaced phases. These hydrocarbons were miscible and they assumed piston-like displacement. An X-ray shadowgraph technique was used to observe the position of the displacing front. Areal sweep efficiencies are plotted versus displacable pore volumes injected for different mobility ratios. In the figure, the x axis is the reciprocal of mobility ratio. Each curve in the graphs corresponds to a specific $t_D / \Delta S$, or displacable pore volume injected. The bottom curves show sweep efficiencies at breakthrough. It is assumed that the displacement has a piston-like front and there is no physical dispersion. Likewise, the porous medium is assumed to be perfectly homogeneous.

For piston-like displacement, the areal sweep efficiency is

$$E_A = A_S / A_T \tag{1}$$

where A_s is the swept area and A_T is the total area. Before and at breakthrough, the amount of displacing fluid injected is equal to the displaced fluid produced, disregarding compressibility. Assuming piston-like displacement, injected volume is related to area swept

$$V_I = A_S \, h \phi \Delta S \tag{2}$$

where V_I is the volume of displacing fluid injected, h is the thickness of the formation, and ϕ is porosity. Hence,

$$E_A = A_S / A_T = V_I / (A_T \, h \phi \, \Delta S) = t_D / \Delta S \tag{3}$$

where $t_D = V_I / (A_T \, h \phi)$ is the pore volume of fluid injected, also commonly called dimensionless time. For $\Delta S = 1$, $E_A = t_D$ before and at breakthrough.

After breakthrough,

$$E_A = (V_I - V_P) / (A_T \, h \phi \, \Delta S) \tag{4}$$

where V_P is volume of displacing fluid produced.

1.3 SIMULATION RESULTS

We use a three-dimensional streamline simulator, called 3DSL, written by Batycky *et al* (1997) to simulate the displacement for the five spot and staggered line drive patterns. In the simulations, we set the conditions identical to those in the experiments and choose relative permeability curves that ensure a piston-like displacement. The conditions are

1. Homogeneous permeability field, *i.e.*, k is constant.

2. Straight line relative permeability curves with end point relative permeability of 1, i.e.,

$$k_{rw} = S_w, \qquad k_{ro} = S_w \tag{5}$$

Therefore, $k_{rw} + k_{ro} = 1$ for any S_w.

4. Mobility is altered by changing viscosity, and the mobility ratio is the reciprocal of viscosity ratio.

5. We set $\Delta S = 1$ which means that ahead of the displacing front, the displacing phase saturation is zero, and behind the front, it is unity.

3DSL is very fast compared to conventional finite difference simulators and exhibits much less numerical dispersion (Batycky *et al*., 1997; Thiele, *et al*., 1996). For our problem, it offers us the streamline distribution which facilitates explanation of displacement behavior.

I use many pressure solves (time steps) and very fine grids (100 by 100 cells for the five spot and 140 by 70 cells for the staggered line drive) to ensure converged simulation results. A grid refinement study (refer to Appendix A for details) showed these grids to be optimal in that further refinement of the grid did not yield noticeable changes in breakthrough time, the oil production curve, or displacement patterns. For unit mobility ratio (M = 1), we actually only need one pressure solve. But for mobility ratios far from 1, we need many pressure solves. For 1/M = 20, we used up to 1000 pressure solves to ensure that the results were converged. In the streamline approach, a pressure solve is accompanied by a re-determination of streamline paths; hence, the flow field.

I also studied the effect of grid orientation on the simulation results (see Appendix B) and found that the pattern behavior is independent of the grid orientation.

Figure 2 displays areal sweep efficiencies as a function of pore volume injected for differing mobility ratios, and compares simulation and experimental results (Dyes *et al*., 1954). The solid lines are simulation results, solid circles experimental results, and dotted lines connect circles for ease of viewing. In this figure, we concentrate on only the favorable mobility ratios, M < 1. We noticed more numerical dispersion for unfavorable mobility ratio cases, not reported here.

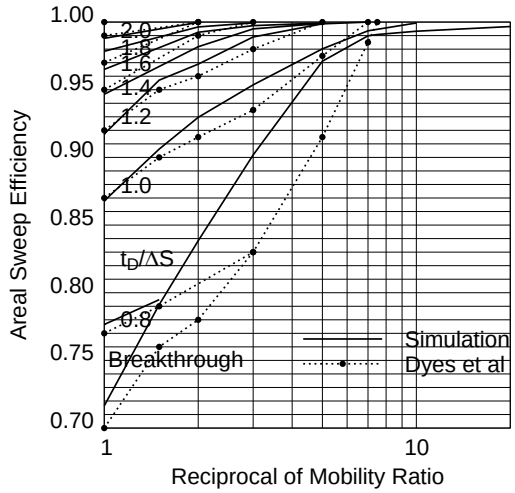

(a) Five Spot Pattern

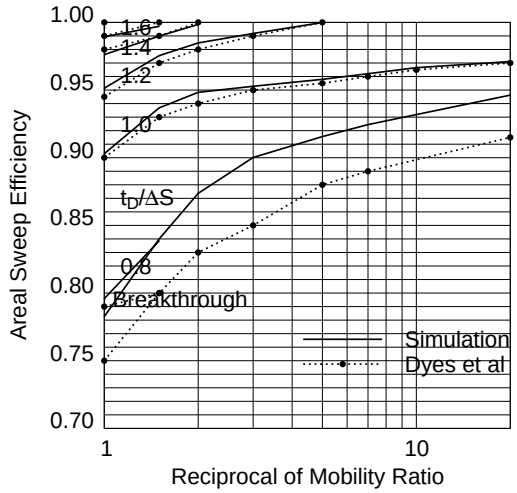

(b) Staggered Line Drive, d/a = 1

Fig 2 Comparison of Simulation and Experimental

Figure 3 shows the displacing fluid fractional flow at the producer as a function of dimensionless time for several mobility ratios. To compute fractional flow from the numerical data we use a central finite-difference formula rather than backward differences. The shapes of the fractional flow curves at breakthrough (t_D from roughly 0.7 to 1) indicate some numerical dispersion. We expect the fractional flow to increase sharply rather than gradually at water breakthrough. As expected, the numerical dispersion decreases as M becomes more favorable (Peaceman, 1977). The most numerical dispersion occurs for unit mobility ratio, as shown in Fig. 3. We modify the breakthrough time by trimming the numerical dispersion as will be described next.

1.4 BREAKTHROUGH DETERMINATION

Due to numerical dispersion, injected fluid breaks through earlier at the producer than it should. However, the numerical dispersion does not have much effect on the late-time displacing fluid production. The fractional flow versus t_D plots shown in Fig. 3 illustrate the early breakthrough caused by numerical dispersion.

To correct for numerical dispersion in breakthrough times and approximate the breakthrough time more accurately, we use fractional flow data after breakthrough and extrapolate back to breakthrough time. A least-squares method is used with second order polynomials:

$$t_D = a + bf_w + cf_w^2 \tag{6}$$

The data points employed lie between $0.1 < f_w < 0.5$. The dashed lines in Fig. 3 illustrate this procedure. All the breakthrough times in Fig 2 are modified using this method.

Numerical dispersion is also related to the number of time steps (*i.e.*, pressure solves). In the streamline approach applied here, dispersion can be introduced through the process of mapping the streamline saturation distribution onto the underlying Cartesian grid used to compute the pressure field[5]. Hence, for a unit mobility ratio where the

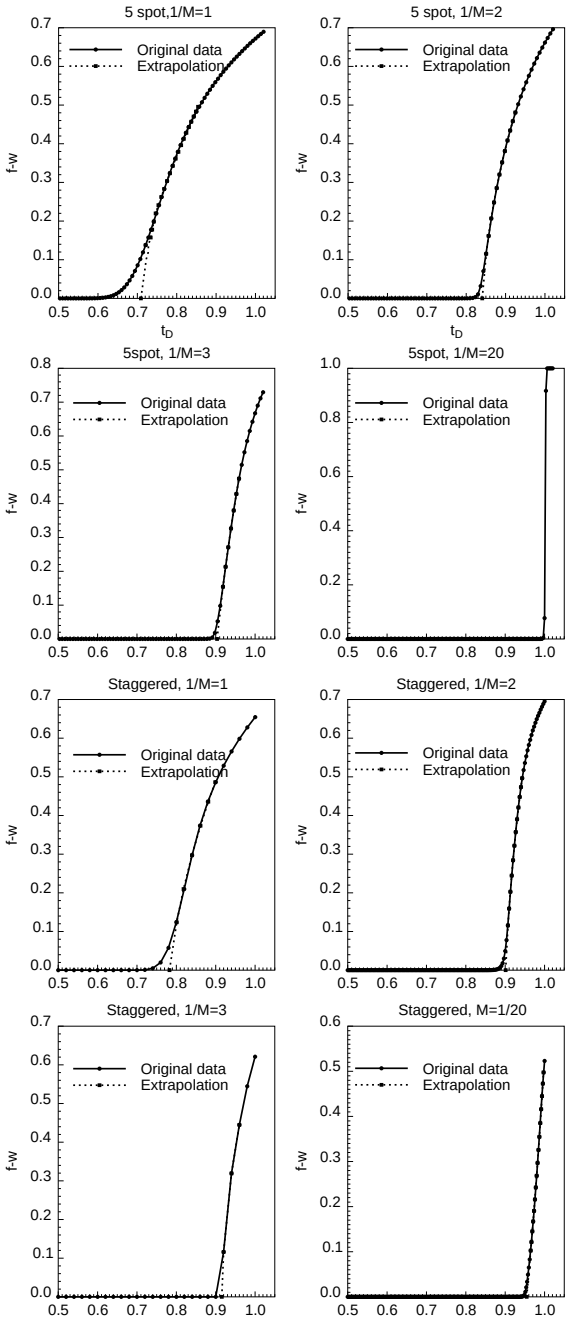

Fig. 3 Fractional Flow(f_w) vs t_D at Producer—Determination of Breakthrough Time

pressure field does not change, the most accurate results are obtained when a single time step is used. By performing various single time step simulations, we determine a breakthrough time of 0.7178 for the five spot with M equal to 1. This is in good agreement with the analytical solution (Morel-Seytoux, 1966) of 0.7177. Likewise, Morel-Seytoux analytically and numerically determined breakthrough times for a staggered-line-drive pattern are both equal to 0.785. With multiple time steps (50) breakthrough times were sooner, but using the method discussed above, we obtain the same values for the breakthrough times, at $M = 1$.

1.5 DISCUSSION OF PATTERN BEHAVIOR

Comparing simulation results and experimental results in Fig. 2, we notice that breakthrough occurs earlier in the experiments than predicted by the simulations. For the staggered-line-drive pattern in Fig 2(b), experimental data indicates that E_A at breakthrough is roughly 0.75 for M equal to 1. In the experiments, there is physical dispersion even though a piston-like front is assumed. In the simulation results presented in Fig. 2a, the sweep efficiency at breakthrough is 99.7% when 1/M = 20. An almost negligible area immediately around the producer is not completely swept at breakthrough due to a very small amount of dispersion in the simulations (refer to Fig. 3, five spot, 1/M = 20).

After breakthrough, the differences in areal sweep efficiencies between the experiments and simulations become much smaller (Fig. 2). After breakthrough, the numerical dispersion consists of only a portion of the displacing fluid produced. As time increases, this portion decreases and the dispersion has less effect on areal sweep efficiency. However, the differences between the experimental results and the simulation results are consistent, i.e. the areal sweep efficiencies of the simulations are generally higher than those of the experiments. As shown in Fig. 2(a), the simulated breakthrough curve levels off at large $1 / M$ with zero slope and does not reach 1 at 1/M = 20. A plot of displacing front position at late displacement time shows that a very small amount of numerical dispersion causes slightly earlier breakthrough. Further details are given in

Appendix C. However, the experimental curve shows E_A equal to 1 at $1/M$ equal to about 7.5. We note that in the plot drawn by Dyes *et al*, the point where the breakthrough curve hits the E_A equal to 1 line is only an extrapolation from other data points.

1.5.1 Areal Sweep Efficiency

Figure 4 plots computed breakthrough, t_D, versus the conventional shape factor d/a for various mobility ratios. The analytical solution for the unit mobility ratio (Morel-Seytoux, 1966) is also plotted on the same figure for comparison. We find a good match of the sweep efficiency at breakthrough between the analytical solution and simulation results.

For unit mobility ratio, Fig. 4 teaches that a staggered-line-drive pattern always has better areal sweep efficiency than a five-spot pattern. As the staggered-line-drive pattern becomes longer relative to its width, the displacement pattern approaches linear flow. High sweep efficiency results.

As the mobility ratio becomes more favorable, the advantage of staggered line drive on sweep efficiency diminishes. When the mobility ratio decreases to 0.2, the five-spot pattern becomes better than the staggered-line-drive pattern with $d/a = 1$. However, if d/a is increased, the staggered line drive recovery is better than the five spot pattern for this mobility ratio.

When the mobility ratio decreases to 0.05 or lower (very favorable), the areal sweep efficiency for the five-spot pattern is very close to 1 at breakthrough. That is, sweep out is complete at breakthrough. At this mobility ratio, the five spot pattern is as good as a very long staggered line drive ($d/a \approx 15$, almost linear flow), and much better than the common staggered line drive ($d/a = 1$). The transition point for five spot sweep efficiency exceeding that from a staggered line drive is around a mobility ratio of 0.3. That is to say, if the mobility ratio is higher than 0.3, a staggered line drive is always better than a five spot. If mobility ratio is lower than 0.3, then the five spot can be higher in sweep efficiency than a staggered line drive.

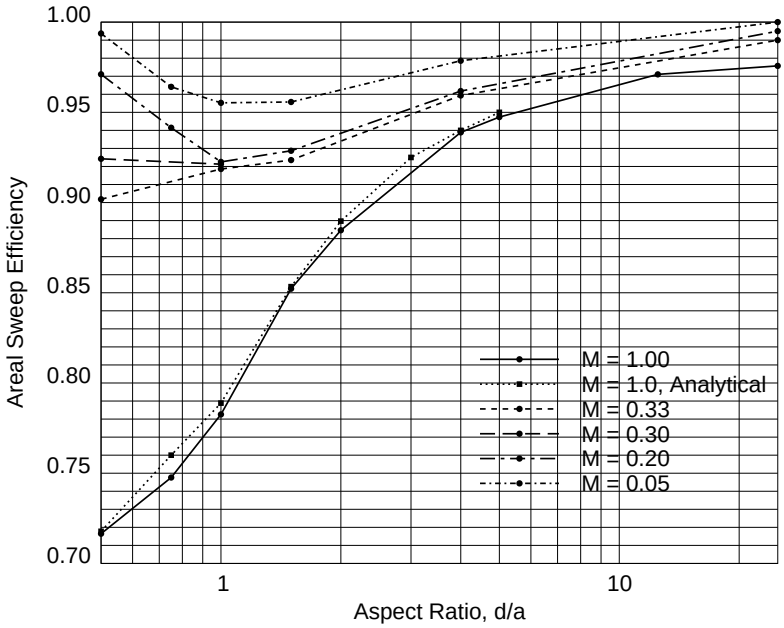

Fig 4 Effect of Mobility Ratios and Patterns
On Areal Sweep Efficiency

The excellent displacement from a five spot pattern for very favorable mobility ratios is explained with the help of streamline distributions. Every pair of streamlines forms a stream tube, and the volumetric flow rate is the same in all the stream tubes. All of the stream tubes connect with the same injector and producer, and the pressure drop for all the streamtubes is the same. With the same pressure drop and the same volumetric flow rate, the flow resistance is the same for all the streamtubes.

For our straight-line relative permeability assumption, we have

$$R_i = -\Delta p / q = \int_0^{L_i} \frac{\mu}{kA} dl \tag{7}$$

where R_i and L_i are the resistance and length of streamtube i, respectively, k is the homogeneous permeability, and A is the cross sectional area of the streamtube. The cross-sectional area is

$$A = hw$$

where h is the constant thickness of the layer and w is the width of the streamtube.

Resistance in streamtube i is the same as that in streamtube j and thus

$$\int_0^{L_i} \frac{\mu}{kA} dl = C \tag{8}$$

for all the streamtubes at a given time, where C is constant. Moving the constant parameters k and h to the right hand side, we have

$$\int_0^{L_i} \frac{\mu}{w} dl = C \tag{9}$$

For a piston-like displacing front,

$$\mu_1 \int_0^{l_{fi}} \frac{1}{w} dl + \mu_2 \int_{l_{fi}}^{L_i} \frac{1}{w} dl = C \tag{10}$$

where μ_1 and μ_2 are the constant viscosity of the displacing and displaced fluids, respectively, and l_{fi} is the distance from the injector to the displacing front.

1.5.2 Unit Mobility Ratio

For a unit mobility ratio, the pressure field remains unchanged throughout the displacement, and so do the streamlines. The streamline distributions at $M = 1$ for the five-spot and staggered-line-drive ($d / a = 1$) patterns are shown in Fig. 5.

For unit mobility ratio, Eq. (10) is

$$\mu \int_0^{L_i} \frac{1}{w}\, dl = C \tag{11}$$

From Eq. 11, we know that if the ith streamtube is longer than the jth streamtube, then the average width of the ith streamtube w_i is greater to maintain the same resistance and flow rate. Therefore, the volume of the ith streamtube is larger than the jth streamtube. The greater the difference in streamtube length, the bigger the difference in streamtube width, and, when breakthrough happens in the jth streamtube, the front has not progressed as far in the ith streamtube.

For a five-spot pattern, the longest streamline is that along the boundary, which is 2a. The shortest streamline is the one along the diagonal, at a length of $\sqrt{2}\, a$. The ratio of the longest streamtube length over the shortest is $\sqrt{2}$. Since the width of the longest streamtube is also $\sqrt{2}$ times as great as the shortest streamtube, the volume of the longest streamtube is twice that of the shortest.

However, for a staggered-line-drive pattern with *d/a* = 1, the ratio of the length along the boundary (3*a*/2) over the diagonal $(\sqrt{5}a/2)$ is $3/\sqrt{5} \approx 1.34$. From the streamline distribution in Fig. 5, we know that the shortest streamline is longer than diagonal, and therefore the ratio of the longest streamline over the shortest is less than 1.34. This ratio is about 1.3 and, therefore, less than that ratio for a five spot pattern which is 1.41. That is to say, the streamlines are more evenly distributed in the staggered

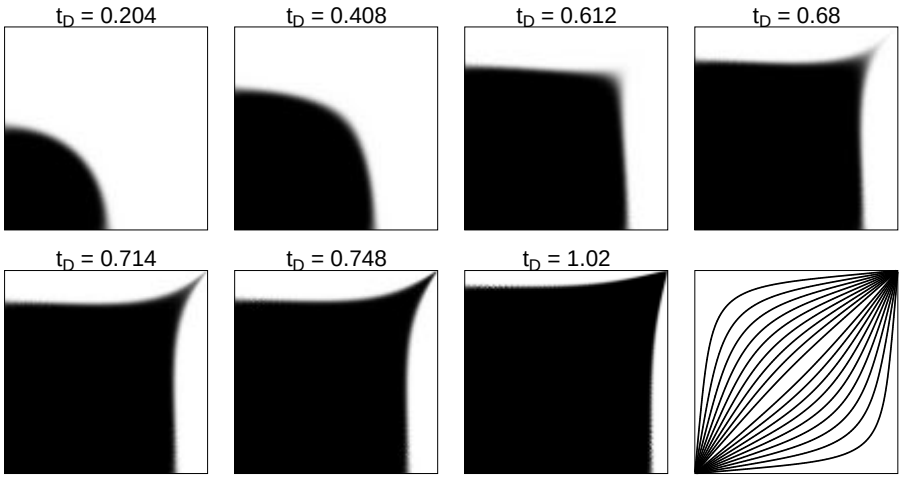

(a) Five Spot Pattern

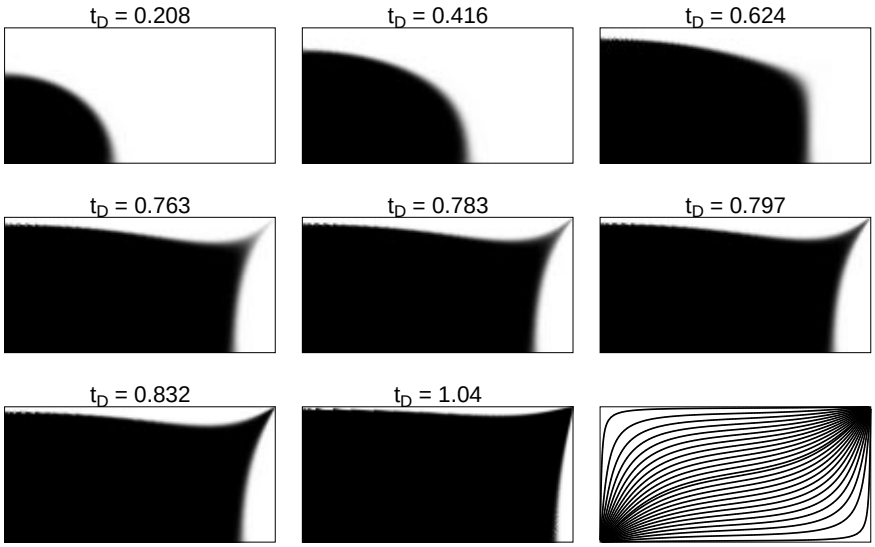

(b) Staggered Line Drive

Fig 5 Saturation and Streamline Distributions, Unit Mobility Ratio

line-drive than in a five-spot pattern. Therefore, when the shortest streamtube breaks through, a larger portion of the other streamtubes have been swept in a staggered-line-drive than in a five-spot pattern. When d/a increases, the streamtube length ratio (longest to shortest) decreases. When breakthrough happens in the shortest streamtube, a greater portion is swept in the longest streamtube resulting in higher sweep efficiency at breakthrough.

1.5.3 Five-Spot Pattern, Very Favorable Mobility Ratio

For a favorable mobility ratio ($M < 1$), the displacement is stable. For equal volumetric flow rate streamtubes, Eq. 10 holds. Here, we consider the case of very favorable mobility ratio, i.e., the displacing fluid viscosity is much higher than that of the displaced fluid. When the front moves a portion of the way down the streamtube, the pressure drop is mainly in the displacing phase. That is to say, after a short injection time (compared to breakthrough), the pressure drop in the displaced phase is negligible. Therefore, Eq. 10 can be simplified to the following form

$$\int_0^{l_{ti}} \frac{1}{w}\, dl \cong C \tag{12}$$

In this extreme case, the displacing phase does not feel the producer until it is very close to it because the pressure drop between the front and the well plays a negligible role in the displacement. Initially, flow around the injector is radial, because the pattern appears to be infinite at short times. For example, examine Fig. 6b for t_D = 0.583. However, after the front reaches a corner of the pattern, the no-flow boundary condition along pattern borders alters the radial flow pattern. Pressure isobars must intersect the no-flow boundaries at 90^o. This constrains the streamlines in the region adjacent to a boundary to be parallel to it. Because the fluids are incompressible, streamlines cannot terminate. The flow field in the region near the front transitions from radial to quasi-radial. From the figure, we also see that streamtubes ahead of the front are narrower along the boundary than those in the center, which makes the front in the boundary streamtubes move faster

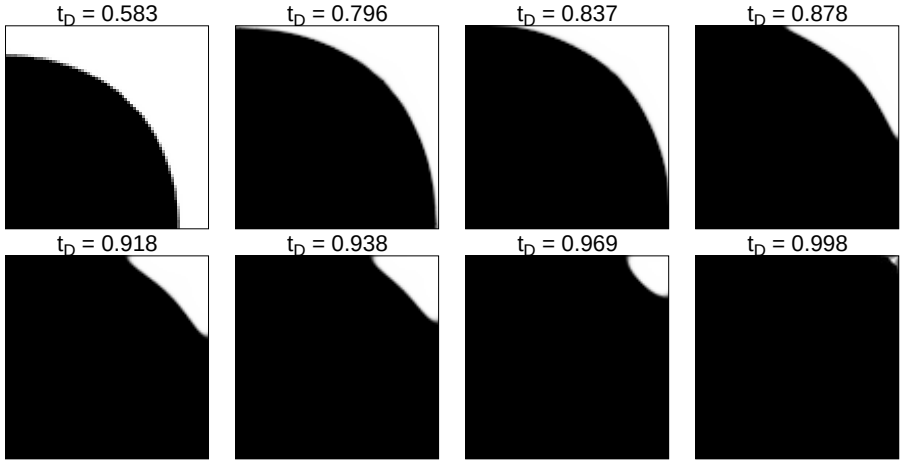

(a) Saturation Distribution

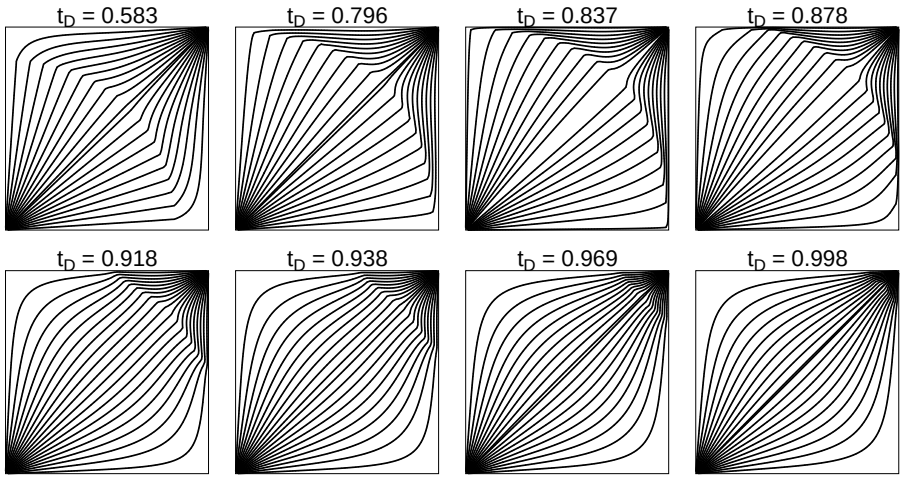

(b) Streamline Distribution

Fig 6 Five Spot Pattern, Very Favorable Mobility Ratio(1/M=20)

than in the central streamtubes. Little area is unswept and the sweep efficiency at breakthrough approaches unity.

Similar to before, when the path of displacing fluid in the ith streamtube is longer than that in the jth streamtube, then the ith streamtube is wider in the swept region to keep the same resistance (same flow rate and pressure). Therefore, the streamtubes along the boundary become wider near the corner where the streamtube changes direction. Streamlines remain smooth. This streamline distribution trend is apparent in Fig. 6b.

In summary, the very favorable mobility ratio conspires with boundary conditions to determine the way that streamlines evolve, and makes the sweep efficiency at breakthrough near unity. If the mobility ratio is very favorable, the pressure drop is mainly in the displacing phase, and it does not feel the well, but is affected by the boundary.

1.5.4 Staggered Line Drive, Very Favorable Mobility Ratio

For the staggered line drive pattern, the displacement at the beginning is similar to that in the five-spot pattern. That is, the displacement pattern is radial around the injector before the front reaches the nearest corner. The differences in displacement behavior between the two patterns occurs after the front reaches the near corner. For a five spot, because of the symmetry, the front reaches the two corners at the same time. However, for a staggered line drive, the front reaches the closest corner first.

After the front passes the near corner, the streamlines evolve in a way similar to the five spot. The streamtubes along the boundary are wide near the corner but narrow near the front. This makes the front near the boundary move faster because the streamtubes are narrower than those in the center of the pattern. Therefore, the front near the boundary on the near no-flow corner side catches up, and the displacement approaches linear flow (see the relevant streamline distribution in Fig. 7 at t_D = 0.60 and 0.80). If the aspect ratio is large, flow in the center of the pattern must become nearly linear because the pressure isobars are nearly straight and intersect the pattern boundary at 90^o.

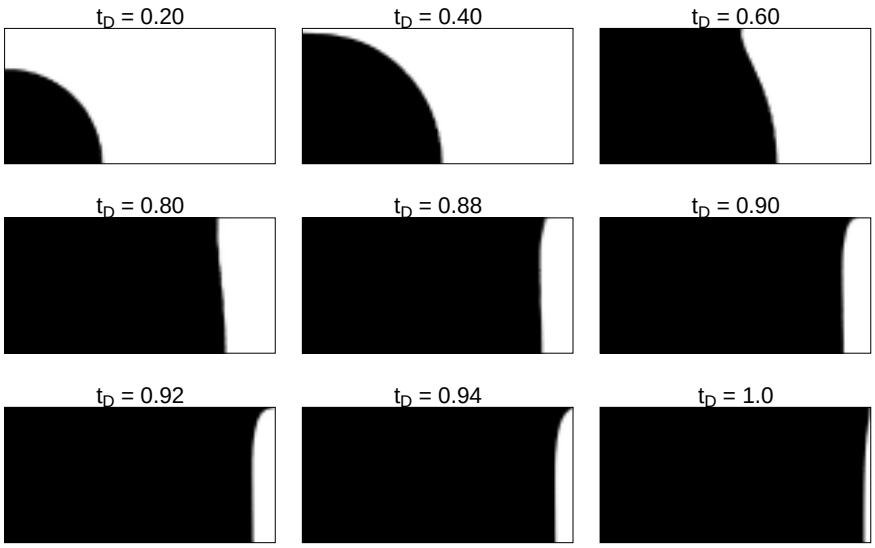

(a) Saturation Distribution

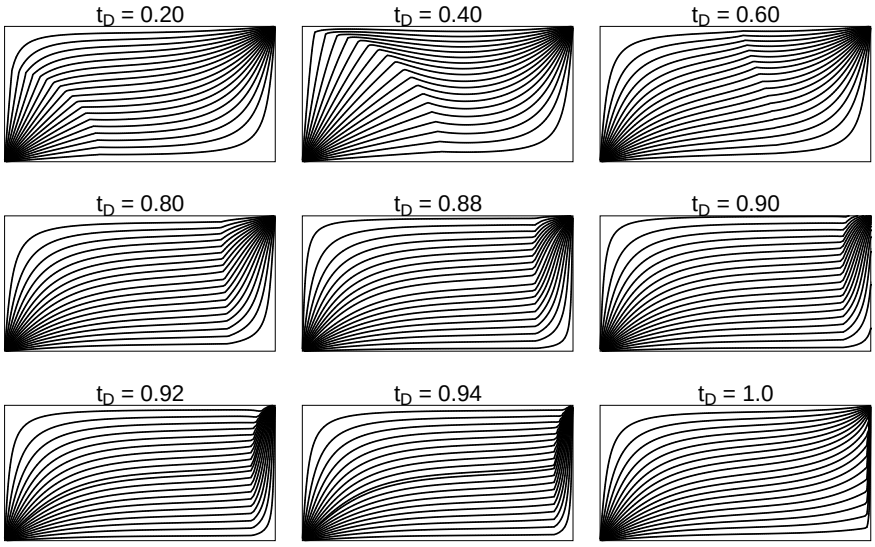

(b) Streamline Distribution

Fig 7 Staggered Line Drive, Very Favorable Mobility Ratio(1/M=20)

Similar to the discussion above for a five-spot pattern, for a very favorable mobility ratio, the displacing front is perpendicular to the borders of the pattern both before and after the front passes the nearest corner. As a result, we see linear displacement for some time until the front on the near-corner side approaches the producer. We see these front shapes in Fig. 7.

When the front approaches the producer, the streamtubes narrow due to the confinement of the pattern boundary and the well. And therefore, with the same flow rate, the displacing fluid will break through relatively quickly in the streamtubes closest to the producer. The front on the far no-flow side progresses more slowly. This streamline distribution does not change greatly as the mobility ratio becomes more favorable. Sweepout of the pattern is not complete at breakthrough. For instance, a small amount of the resident fluid remains along the right hand boundary as shown in Fig 7a at $t_D = 0.94$.

If the length of staggered line drive is increased (increasing d / a), then the displacement will approach linear flow and the sweep efficiency will approach unity. The proportion of unswept area decreases as d / a increases.

1.6 CONCLUSIONS

Pattern performance changes with mobility ratio. For unit mobility ratio, unfavorable mobility ratios and some favorable mobility ratios $(M > 0.3)$, a staggered-line-drive pattern has higher areal sweep efficiency than a five-spot pattern. However, for very favorable mobility ratios $(M < 0.3)$, a five-spot pattern has better sweep efficiency than a common staggered-line-drive.

The reason for this behavior is the change of streamline and pressure distributions with mobility ratios. For very favorable mobility ratios, the displacing front is near an isobar and intersects the pattern boundary at 90^o. This causes the fronts at times near breakthrough to become radial around the producer for a five-spot pattern. This displacing front shape is due to the symmetry of the five spot pattern.

For a staggered line drive, the displacing front is also perpendicular to the border of the pattern. However, because the pattern is not symmetric, sweepout at breakthrough is not complete. Only in the limit of very large d/a will the areal sweep efficiency approach 1.

The simulation results are quite close to the analytical solutions for unit mobility ratio. The results are also very close to the experimental data, Dyes *et al.* (1954), after breakthrough at various mobility ratios. We find physical dispersion in the Dyes *et al.* experimental results that cause earlier breakthrough time.

We observed some numerical dispersion in our simulation results. For very favorable mobility ratios, the dispersion is small. We corrected the simulation results by fitting the fractional flow curve with a second order polynomial to estimate breakthrough time.

Appendix A—Effect of Grid-Block and Time-Step Size

The number and size of grid blocks and time steps has a strong effect on simulation results. The extent of the effect is related to the mobility ratio. This study is performed on five-spot pattern cases and the results are shown in Fig. A. However, the conclusions drawn from this study do not lose any generality.

A.1 EFFECT OF TIME-STEP SIZE

Figure A plots the fractional flow at the producer versus time; changes in this curve versus the number of grid blocks or time step are a convenient measure of the accuracy of a solution. Comparing the effect of time-step size between M=1 and M=1/20 in Fig A, it is obvious that the effect of time-step size is much stronger in the very favorable mobility ratio case (M=1/20). For unit mobility ratio (M=1), simulation results stop changing at 50 time steps. However, for M=1/20, the difference between simulation results and the converged solution for the same number of time steps is much greater. The reason is described below.

For unit mobility ratio, the pressure field as well as the streamline distribution does not change with time. If we map the analytical solution along the streamline, then, time-step size does not have any effect on the simulation result. However, I mapped the numerical solution to be consistent with the very favorable mobility rstio cases in which mapping the analytical solution is not applicable.

As mobility ratio departs from unity, the pressure field changes more intensively. For a very favorable mobility ratio, we must solve the pressure field enough times to get a converged solution. We can see that, for M=1/20, the simulation result converges at 100 pressure solves (time steps).

For the calculations presented in the main portion of the report, I used 100 time steps for unit mobility ratio and 300 time steps for M=1/20. The simulation result is converged in terms of number of time steps.

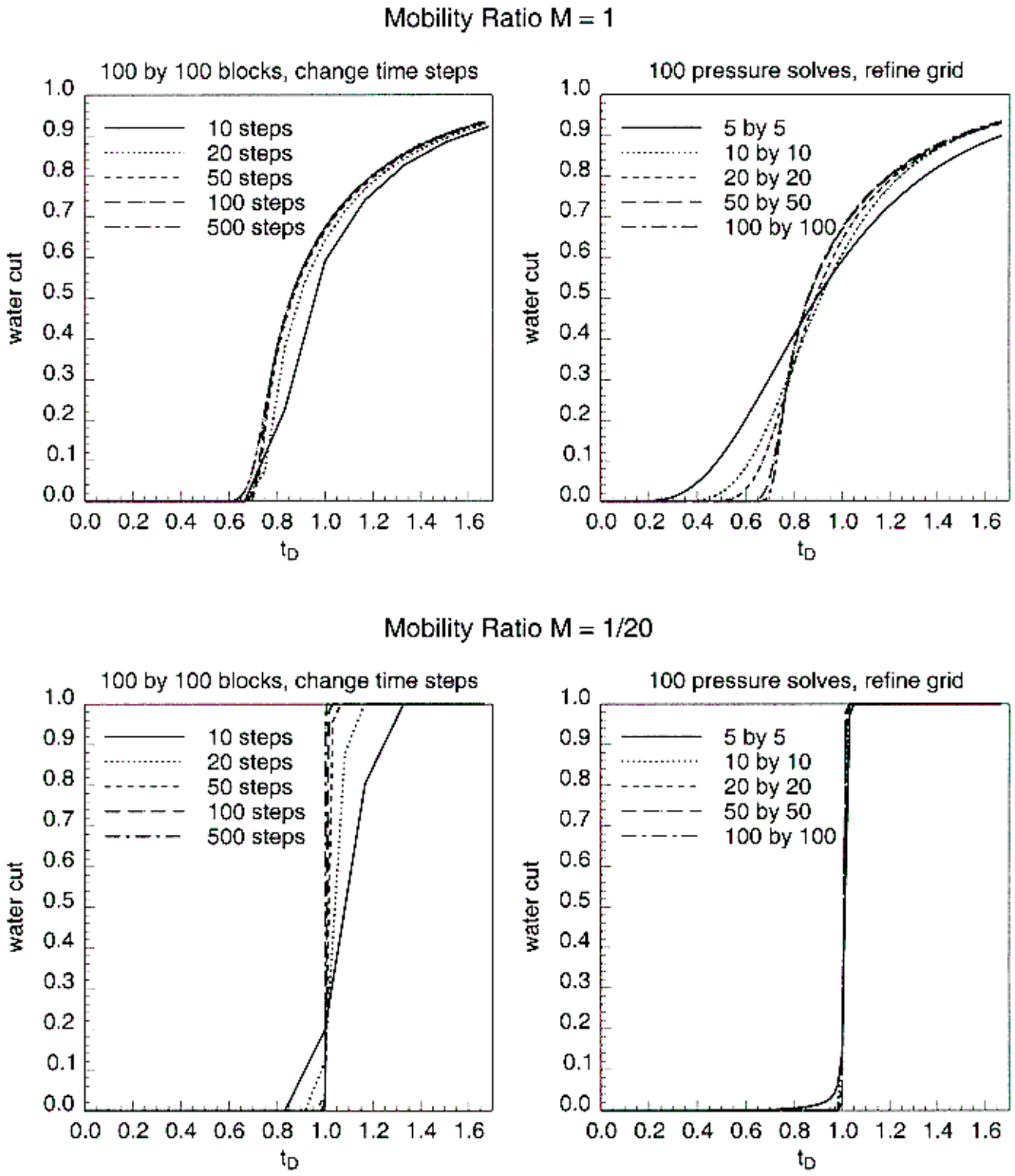

Fig. A Effect of Refining Grid and Increasing Time Steps on the Simulation Accuracy

A.2 EFFECT OF GRID-BLOCK AND TIME-STEP SIZE

Figure A also shows that the effect of grid-block size is much stronger in the unit mobility ratio cases than it is in the very favorable mobility ratio cases. For M=1/20, the simulation results converge when the number of grid blocks is greater than 10 by 10. However, for unit mobility ratio, results converge for much finer grid blocks (100 by 100).

In very favorable mobility ratio cases, the simulation result is not sensitive to the grid-block size. The reason can be the very sharp displacing front for very favorable displacement.

I used 100 by 100 grid blocks for all the cases in this study, and therefore, the simulation results are converged in terms of grid-block size.

A.3 CONCLUSION

In the unit mobility ratio cases, simulation results are sensitive to the grid-block size but not very sensitive to time-step size. In the very favorable mobility ratio cases, the simulation results are sensitive to grid-block size. For the calculations presented in the main portion of the report, I used enough number of time steps and grid blocks for a converged simulation result. Therefore, the results above demonstrate that simulations are free from effects of the size of grid blocks and time steps.

Appendix B—Effect of Orientation of Grid-Blocks

We thought that the orientation of the grid-block with respect to the flow direction may affect the simulation results, especially the streamline distribution. Therefore, I studied this effect. In the work presented before, the injector and producer are aligned with the diagonal as shown in Fig. B1a. It was not clear whether the streamline distribution changes if streamlines align with the grid block (see Fig. B1b). Again, I only studied the five-spot pattern. However, the conclusion is general for other patterns.

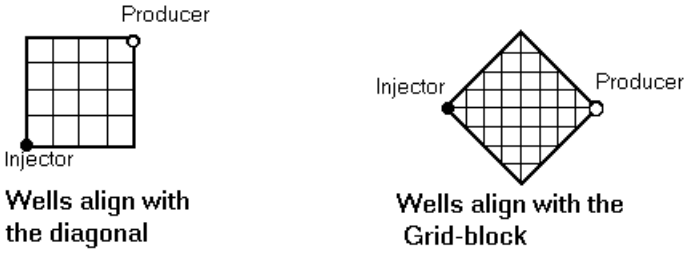

(a) (b)

Fig. B1 Grid Orientation.

I ran the simulation for both cases illustrated in Fig. B1 with time steps and grid-block size remaining the same.

In 3DSL only rectangular grid blocks can be used, in the rotated grids. Therefore, I have a bigger domain with the quarter of five-spot pattern sitting in the middle. A very low permeability was assigned to regions outside the five-spot domain. In doing so, there is essentially no flow outside the five-spot domain. The no-flow boundary is approximated by zigzag lines along the boundary. However, as I used many grid blocks(100 by 100), the boundary is quite smooth.

Because the grid block in the no-flow corner is closed on three sides, it is not open to flow and it is not filled with the displacing phase when the surrounding blocks in the five-spot pattern domain are swept by the displacing phase (see Fig. B2). It causes the breakthrough time to be slightly earlier (about 0.1%). However, it does not make much difference to the overall pattern behavior.

There is also some dispersion into the region outside the five-spot domain, as illustrated in Fig. B2, due to the nonzero permeability in that region. 3DSL does not work for zero permeability. This dispersion is small and does not affect the pattern behavior.

Comparing Fig. B2 with Fig. 6, we can easily see that the direction of the grid does not effect the pattern behavior. Therefore, any difference in the pattern behavior at different mobility ratios is not due to improper grid orientation.

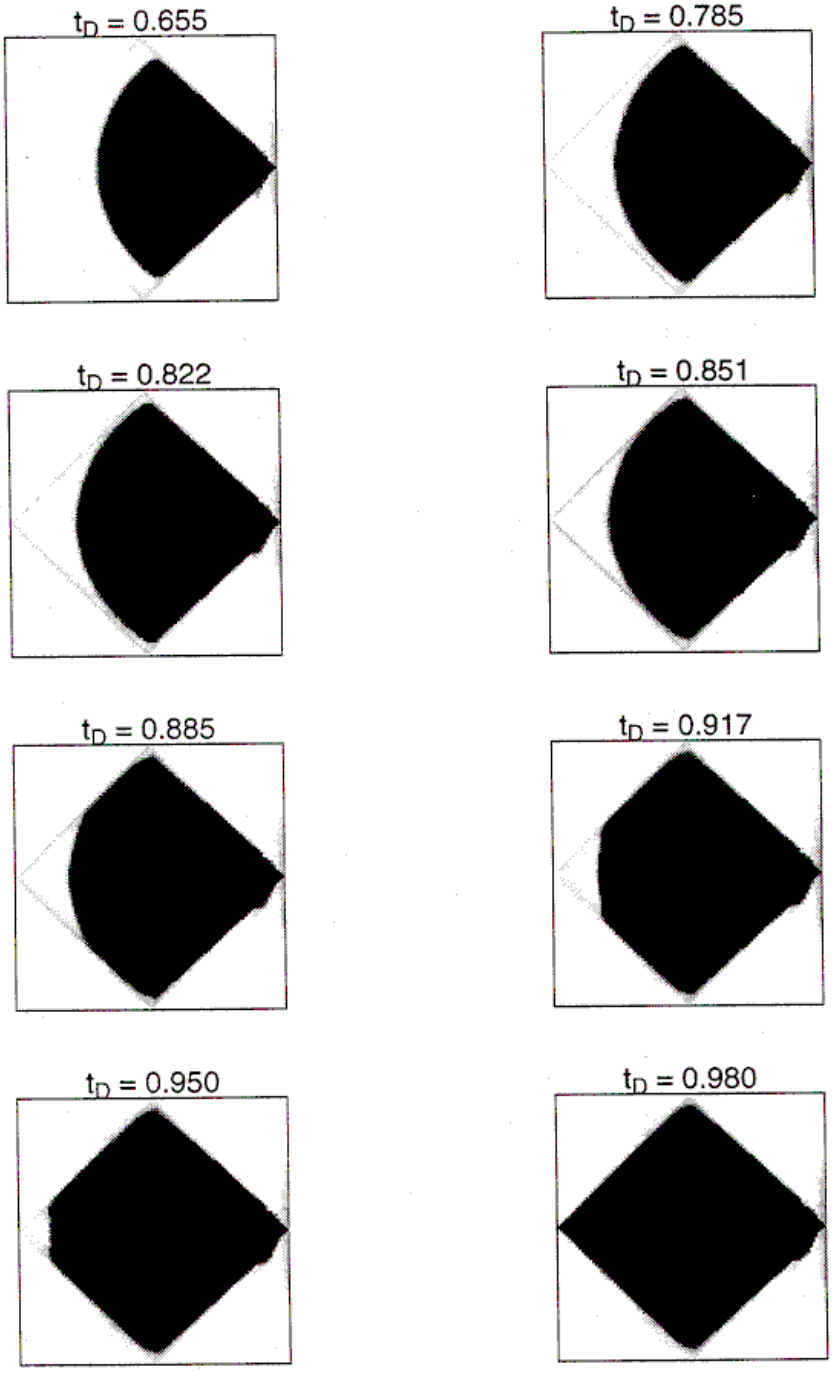

Saturation Distribution

Fig B2 Five Spot 1/M = 20.0

Appendix C—Numerical Dispersion

Fig. C shows the position of the displacing front at times near breakthrough (t_D = 0.95) for the case of a five-spot pattern and a very favorable mobility ratio, M=1/20. The solid line plots front location in the streamline closest to the boundary, whereas the dashed line corresponds the diagonal line between injector and producer. The purpose of this plot is to study the numerical dispersion for this case, because we think that the breakthrough time should be unity in the absence of numerical dispersion.

I assumed piston-like displacement in choosing relative permeability curves. However, because I mapped the numerical solution along the streamlines, this sharp front may be smeared by numerical dispersion. However, due to the numerical-sharpening effect for very favorable mobility ratios, the front is still quite sharp.

From Fig. C, it is obvious that the displacing front is very sharp. However, we can still clearly see that it is not exactly a piston-like displacement due to the numerical dispersion. The dispersion is very small. If there is no dispersion, the piston-like displacing front bisects the numerically predicted front. The dimensionless width of the front is 0.02, and the perfect piston-like front is in the middle. A dimensionless distance of 0.01 from the front in the simulation result. Therefore, the numerical dispersion causes 0.01 (t_D) earlier breakthrough in the earliest breakthrough streamline. Referring to Fig. 2(a), the calculated breakthrough t_D for this case is over 0.99. Therefore, without numerical dispersion, there will be perfect displacement for the five-spot pattern at very favorable mobility ratio.

Fig. C also tells us the front shape along the boundary is almost the same as that along the diagonal. Therefore, the slanted front is only due to the numerical dispersion, not the boundary effect.

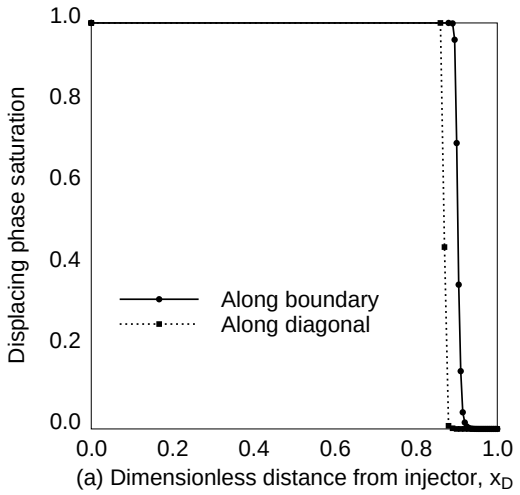

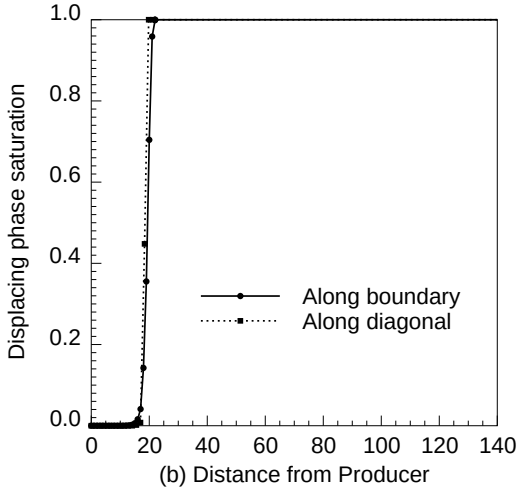

Fig. C Displacing Front

Five Spot Pattern, 1/M = 20

2 STREAMLINES TO SOLVE INVERSE PROBLEMS

2.1 DEFINITION OF THE RESEARCH TOPIC

The proposed research is to apply the concept of streamlines to infer permeability fields based on the tracer breakthrough curve and pressure differences between the injector and producers. The basic idea of my approach is to adjust the streamlines to match the reference fractional flow and pressure data, and through streamlines to modify the underlying permeability field.

Because there is no flow across a streamline, we can represent the flow field by 1D flow streams along the streamlines. Each streamline is associated with a time of flight which indicates the breakthrough time. In the 3DSL streamline simulator (Batycky *et al*), we solve the pressure field at given saturation distribution, obtain the streamline distribution, then map the Buckley-Leverett solution along the 1D streamlines for a short time period, and then solve the pressure field again and repeat the process. Because the pressure equation and saturation equation are decoupled in 3DSL, the simulation is speeded up significantly.

Conventional reservoir simulation history matching is time consuming because of the large number of grid blocks. However, if we know the time of flight of the streamline, then we will know the breakthrough time of an individual streamline. Therefore, if the breakthrough curve for our computed permeability field does not match the reference breakthrough curve, then we know along which streamline and in which way to modify the permeability for a better match.

This approach is described below. To start with this project, I made the following simplifications:

- Incompressible flow, because the streamline simulator (3DSL by Batycky et al) that I am using works for incompressible fluid flow only;
- Piston-like displacement;
- Unit mobility ratio, valid for tracer flow study;

- Two dimensional;
- No constraint of the permeability value or its distribution.

Steps of the Streamline Approach to the Inverse Problem:

1. Given a reference permeability field, use the 3DSL streamline simulator for forward simulation to obtain the reference water breakthrough curves at producers and pressure drops between injector and producers.
2. Start from an initial uniform permeability field. Do the same simulation. Check the match—both breakthrough and pressure drop. If it does not match the reference data, modify the permeability as in the following steps;
3. Work on the streamlines: Calculate the time of flight for all streamlines using 3DSL to output the coordinates of the streamlines. Sort the streamlines in the order of time flight.
4. Compare the computed and the reference breakthrough and pressure drops. For the breakthrough curve, check where in the curve the difference lies. Relate it to the corresponding streamline, and then change the permeability value depending on the difference of the breakthrough curves;
5. Repeat the simulation using the new permeability distribution. This completes one iteration;
6. Repeat steps 2 to 5 until the match is good enough.

I obtained very promising results with this approach. In the reference field, there are one injector and two producers. Between the injector and producer there exists a high permeability channel, and between the injector and producer 2 there is a low permeability barrier (See Fig. 1). Starting from a homogeneous permeability field, both the breakthrough and pressure drops are far away from the reference (see Fig. 2). After three iterations, I obtained a very good match both in pressure drops and breakthrough curves (Fig. 2), which indicates that this approach converges very fast, much faster than most of other approaches to this inverse problem.

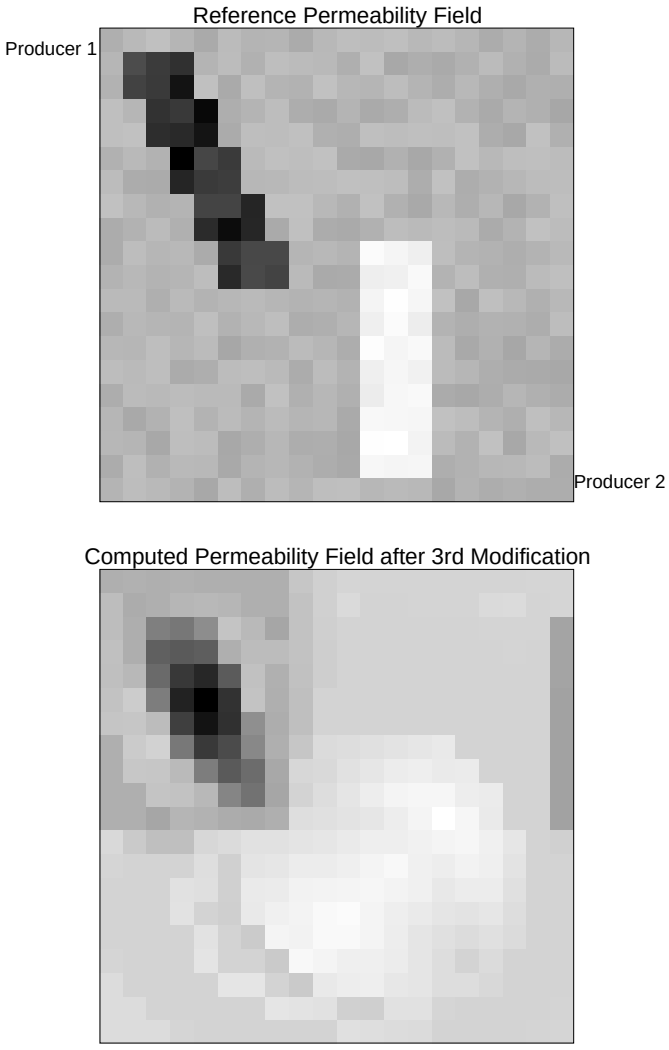

Fig. 1 Comparison on Permeability Field

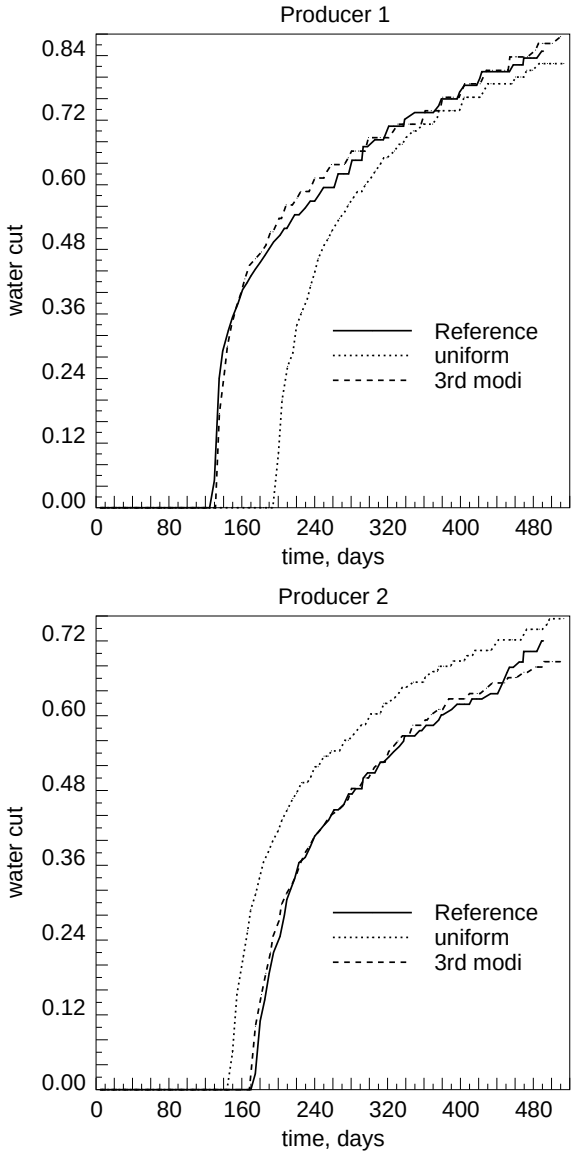

Fig. 2 Comparison on Breakthrough Curve

Fig. 3 plots the error versus the number of iterations. The error is defined as

$$E = \sum_{i=1}^{n\_prod} \left[E_{fw,i} + E_{\Delta p,i} \right] \tag{1}$$

where E_{fw} is the average absolute error in the fractional flow at different times, and $E_{\Delta p,i}$ is the relative error of the pressure drops between the injector and producers at producer i. They are defined below

$$E_{fw,i} = \frac{1}{n} \sum_{j=1}^{n} \left| f_{w,i,j}^{C} - f_{w,i,j}^{R} \right| \tag{2}$$

where $f_{w,i,j}^{C}$ and $f_{w,i,j}^{R}$ are the computed and reference water fractional flow during time step j at producer i, respectively.

$$E_{\Delta p,i} = \left| \frac{\Delta p_i^C - \Delta p_i^R}{\Delta p_i^R} \right| \tag{3}$$

where Δp_i^C and Δp_i^R are calculated and reference pressure drop between the injector and producer i, respectively.

I normalize the error in pressure by the reference pressure so that it will be within the range of 0 to 1 and it is of the same scale as the error in fractional flow. Then I can sum up them up to have a unified error estimation.

The solid line in Fig. 3 (a) is the sum of error at the two producers. The dashed and dotted line are for each producer, respectively.

Comparing the computed permeability field with the reference field in Fig. 1, we find that, with this approach, the high permeability channel is retrieved quite accurately. For the barrier, the resolution is not very good. However, we have good matches for the breakthrough curve and pressure drop.

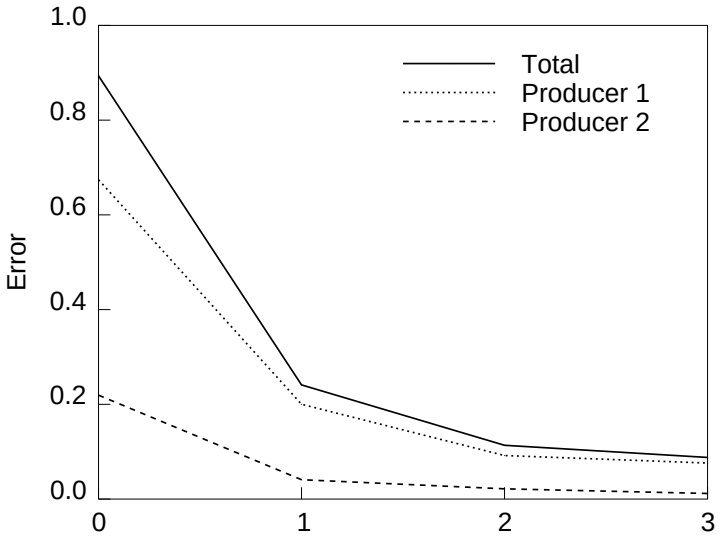

(a)

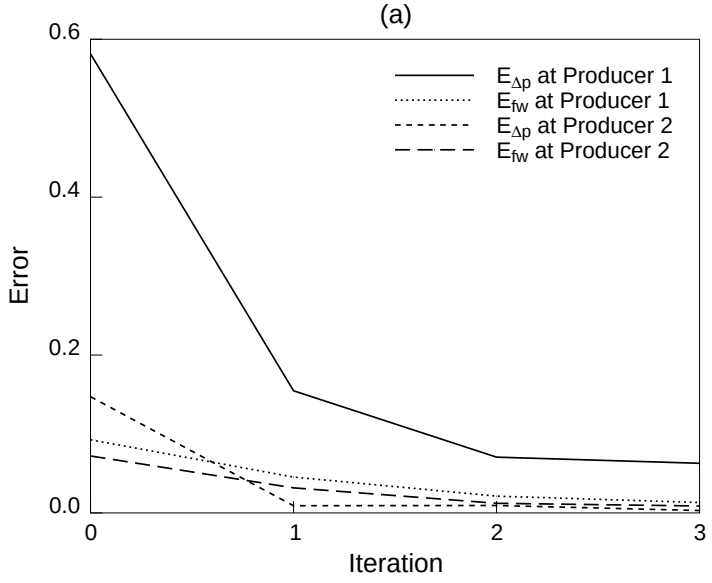

(b)

Fig. 3 Error vs Iterations

2.2 IMPORTANCE OF THE RESEARCH

History matching plays an important role in reservoir engineering. It is important for prediction and data interpretation. In many cases, we have water or tracer breakthrough and pressure information at the producers. This information contains much information about the permeability distribution of a reservoir, but it is difficult to infer this distribution. There are many approaches to this inverse problem. Most approaches manipulate parameters at the grid-block level that corresponds to conventional simulation grids. Because there are many cells, the optimization problem is large. By conducting the optimization at the streamline level, the opportunity for speed improvement is great. Since we know how each streamline affects water cut, we can speed up the inverse process tremendously. A more typical approach would be to perturb parameters in a more random fashion to gauge the effect of the parameter.

2.3 FUTURE WORK PLAN AND EXPECTED RESULTS

There are many simplifications in my current study. Simplification means limitations in the application. Therefore, my future work will be focused on relaxing the simplifications to broaden its application. My plan is to

- Release the piston-like displacement and unit mobility ratio assumptions. It is not difficult to do since I can simply map the Buckley-Leverett solution instead of the sharp front, and I can map the numerical solution for one-dimensional displacement instead of the analytical one along the streamline.
- Seek a streamline simulator for compressible flow. Study my current method for modifying a permeability field to see whether it is still valid for compressible flow. Also study what modification of the current approach should be made for compressible flow. Then I can make this approach work for primary recovery and well-test problems. This will be the most difficult portion and therefore the key part of this project.

- Put constraints on the permeability distribution from other information such as seismic data, and broaden its use to three-dimensional problems. Improve the method.
- For comparison, develop examples that use a conventional history-matching approach to infer heterogeneity.

I will continue to work on this topic in my Ph.D. When this project is finished, I expect that this approach will work for very general history matching purposes.

NOMENCLATURE

A	area, L^2
A_S	area swept, L^2
A_T	total area of the pattern, L^2
a	distance between like wells (injection or production) in a row, L
d	distance between adjacent rows of injection and production wells, L
E_A	areal sweep efficiency
f_w	fractional flow of water
h	bed thickness, L
k	permeability, L^2
k_{ro}	relative permeability of oil
k_{rw}	relative permeability of water
l	length, L
L_i	length of stream tube i, L
l_{fi}	distance of the displacing front from the injector in stream tube i, L
M	mobility ratio
p	pressure, $M/L \bullet T^2$
q	flow rate, L^3/T
R_i	flow resistance of stream tube i, $M/L^4 \bullet T$
S	saturation
S_w	water saturation
t_D	dimensionless time
V_I	volume of displacing phase injected, L^3
w	width of a stream tube, L
ϕ	porosity
μ	viscosity, $M/L \bullet T$

REFERENCES

1. Batycky, R. P., Blunt, M. J., and Thiele, M. R.: "A 3D Streamline-Based Reservoir Simulator" SPE Reservoir Engineering, 12, 246, (1997).

2. Craig, F. F. Jr.: "The Reservoir Engineering Aspect of Water Flooding," Society of Petroleum Engineers Monograph, Dallas, TX, 1971.Dyes, A. B., Caudle, B. H., and Erickson, R. A., "Oil Production after Breakthrough—as Influenced by Mobility Ratio", Petroleum Transactions, *AIME*, 201, 27 (1954).

3. Dyes, A.B., Caudle, B.H., and Erickson, R.A.: "Oil Production After Breakthrough—as Influenced by Mobility Ratio," Petroleum Transactions, AIME, 201, 27 (1954).

4. Lake, L. W.: Enhanced Oil Recovery. Prentice Hall Inc., New Jersey, 1989.

5. Morel-Seytoux, Hubert J.: "Unit Mobility Ratio Displacement Calculations for Pattern Floods in Homogeneous Medium," SPE J, 6, 217, (1966).

6. Peaceman, D. W., Fundamentals of Numerical Reservoir Simulation. Elsevier Scientific Publishing Co., New York, 1977.

7. Thiele, M. R., Batycky, R. P., Blunt, M. J. and Orr Jr, F. M. Jr.: "Simulating Flow in Heterogeneous Systems Using Streamtubes and Streamlines," SPE. Reser. Eng, 11, 5, (1996).